Giant monopole strength in ^{58}Ni

Y.-W. Lui, H. L. Clark, and D. H. Youngblood
Cyclotron Institute, Texas A&M University, College Station, Texas 77843
(Received 3 November 1999; published 19 May 2000)

The strength distribution of the giant monopole resonance in ^{58}Ni has been measured from $E_x = 10$ to 35 MeV using small-angle scattering of 240-MeV α particles. $E0$ strength corresponding to 74^{+22}_{-12}% of the $E0$ EWSR was found between $E_x = 12.0$ and 31.1 MeV with a centroid of $20.30^{+1.69}_{-0.14}$ MeV.

PACS number(s): 24.30.Cz, 25.55.Ci, 27.40.+z

Previously, using inelastic scattering of 240-MeV alpha particles at small angles with a deformed potential analysis, we reported [1] 32% of the $E0$ EWSR in two Gaussian peaks in ^{58}Ni and argued that no more than 50% of the $E0$ strength was located between $E_x = 12$ and 25 MeV. Satchler and Khoa [2] carried out a folding analysis of our data and on that basis concluded the two peaks contained $\sim$50% of the $E0$ EWSR. The location of the remainder of the $E0$ strength in ^{58}Ni was a puzzle. We have again measured the $E0$ strength in ^{58}Ni, this time using a detector that extends the measurement up to $E_x = 60$ MeV, compared to $E_x \leqslant 30$ MeV in the previous measurement, in order to locate strength at higher excitation and we report those results here.

A 240-MeV α-particle beam from the Texas A & M K500 superconducting cyclotron was used to bombard a 4.02-mg/cm^2 ^{58}Ni metal foil located in the target chamber of the multipole-dipole-multipole spectrometer. Inelastically scattered α particles were detected in the focal plane detector that measured position and angle in the scattering plane. The out-of-plane scattering angle ϕ was not measured. Position resolution of approximately 0.9 mm and scattering angle resolution of about 0.09° were obtained. The detector covers the range $E_x = 7-62$ MeV. The experimental technique and the detector have been described in detail in Refs. [3–5].

Data were taken with the spectrometer at 0.0° ($0.0° < \theta < 2.0°$) and at 3.5° ($1.5° < \theta < 5.5°$). Each data set was divided into ten angle bins, each corresponding to $\delta\theta \approx 0.4°$ using the angle obtained from ray tracing. ϕ is not measured by the detector, so the average angle for each bin was obtained by integrating over the height of the solid angle defining slit and the width of the angle bin. Cross sections were obtained from the charge collected, target thickness, dead time, and known solid angle.

Uncertainties in target thickness, solid angle, etc. result in about a $\pm$10% uncertainty in absolute cross sections. The target thickness was measured by weighing and checked with the energy-loss technique using the 240-MeV α-particle beam. A spectrum obtained in the present experiment is compared to the earlier data [1] in Fig. 1. Except for a somewhat larger background at lower excitation in the earlier data, they are in excellent agreement up to the $E_x = 30$ MeV limit of the earlier data.

Multipole strength distributions were obtained using ''slice analysis'' [3,4] where a continuum is estimated and subtracted, leaving a giant resonance peak. This peak is then divided into several intervals and cross sections obtained for each interval. The resulting angular distributions are then fit with distorted-wave Born approximation (DWBA) calculations for various multipoles. The determination of the uncertainties in such a fit process are described in Ref. [3]. From the results obtained for ^{24}Mg [3], ^{28}Si [4], and ^{90}Zr [6], the shape of the $E0$ strength distribution is not necessarily Gaussian, therefore the Gaussian peak fitting analysis reported for the earlier ^{58}Ni data was not used here.

The spectrum shown in Fig. 1 reveals that giant resonance strength extends from $E_x = 10$ MeV to $E_x \approx 35$ MeV in ^{58}Ni, similar to what was seen in ^{28}Si [4] and ^{24}Mg [3]. The estimated continuum is indicated in Fig. 1 by the solid line, with the area above this line corresponding to the giant resonance peak. This peak was then divided into 15 intervals varying from 1 to 3 MeV in width and cross sections obtained for each interval. Samples of the angular distributions obtained for the giant resonance peak for two different excitation intervals are shown in Figs. 2(a) and 2(b). The angular distributions obtained for the continuum changed only slightly over the excitation range and the distribution for one excitation interval is shown in Fig. 2(c).

Inelastic scattering folding model calculations were performed following the method of Satchler and Khoa [2] using density-dependent single folding with a Woods-Saxon imaginary term and were carried out with the computer code PTOLEMY [7]. Input parameters for PTOLEMY were modified [8] to obtain a correct relativistic calculation. The shape of

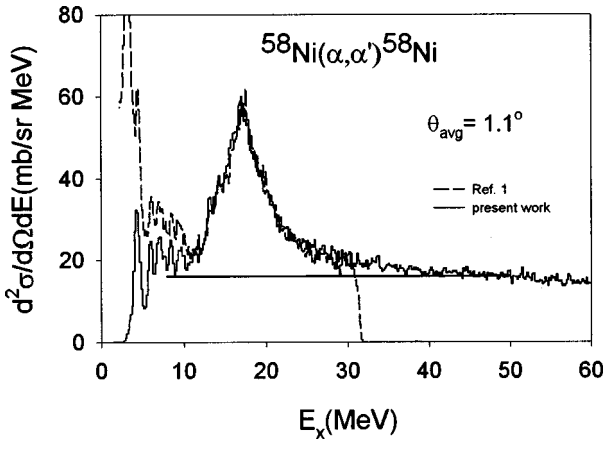

FIG. 1. Inelastic α spectra from two different experiments for ^{58}Ni. The solid straight line indicates the separation chosen between the giant resonance peak and the continuum. A spectrum from the work described in Ref. [1] is shown by the dashed line, while the spectrum from the present work is shown by the solid line.

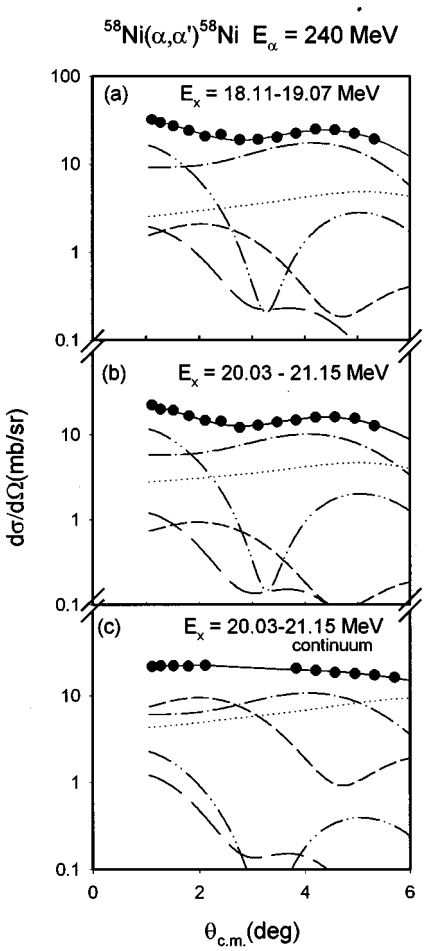

FIG. 2. (a),(b) Angular distributions of the differential cross section for inelastic α scattering for two excitation regions of the giant resonance peak. (c) Same for the continuum. The solid lines are the DWBA calculations for the sum of all the distributions of the multipoles. The dashed–double-dotted line shows the $L=0$ component, the short dashed line shows the $L=1$ component, the dashed-dotted line shows the $L=2$ component, the dotted line shows the $L=3$ component, and the long dashed line shows the isovector $L=1$ component. When not shown, the error in the data is smaller than the data points.

the real parts of the potentials and form factors for PTOLEMY were obtained using the codes SDOLFIN and DOLFIN [9]. The transition densities and sum rules for various multipolarities followed the expressions in Ref. [10]. Radial moments for ^{58}Ni were obtained by numerical integration of the Fermi mass distribution with $c=4.08$ fm and $a=0.515$ fm [10]. Folding model parameters were obtained [11] from elastic scattering data of ^{58}Ni$+\alpha$ at 240 MeV extending from c.m. angles of 2°–34° and are listed in Table I.

The angular distributions of the cross sections for each energy bin were fit with DWBA calculations corresponding to isoscalar $L=0$, 1, 2, 3, and 4 strength. The isovector dipole was also included in the calculation using the strength distribution obtained from photonuclear work [12]. A similar analysis for the continuum was also performed to extract giant monopole resonance (GMR) strength. Strength distributions for other multipoles cannot reliably be obtained for the continuum [3]. Fits obtained are shown superimposed on the data in Fig. 2.

TABLE I. Folding model parameters used in the DWBA calculations. R_P and R_T are the Coulomb radius parameters for projectile and target, respectively.

V (MeV)	W (MeV)	r_i	a_i (fm)	R_P	R_T
41.19	40.39	0.821	0.974	1.336	1.256

The $E0$ and $E2$ strength distributions obtained from the slice analysis are shown in Figs. 3(a) and 3(b). The $T=0$ $L=1$ strength obtained corresponds to $\approx$41% of the isoscalar $E1$ EWSR and was spread more or less uniformly from $E_x=12$ to 35 MeV. Due to the limited angle range of the experiment $L=3$ and higher multipole strengths could not always be unambiguously separated. The $L\geqslant 3$ strength extended smoothly from $E_x=18$ to 34 MeV.

$E2$ strength corresponding to $115\pm 18\%$ of the $E2$ EWSR was found between $E_x=10$ and 20 MeV with a centroid of 16.1 ± 0.3 MeV and rms width of 2.4 ± 0.2 MeV. The centroid and widths of the $E2$ distribution are in good agreement with previous measurements [1,13], but the total strength reported previously was lower ($58\pm 8\%$ [1] and $58\pm 12\%$ [13]). Satchler and Khoa showed that the deformed potential model (used in Refs. [1] and [13]) gives a cross section approximately 20% higher than the folding model, which would increase the sum rule fraction seen in the earlier experiments to about $70\pm 10\%$, still lower than obtained here. The large excitation range covered in the present data revealed giant resonance strength beyond the $E_x=30$ MeV limit of the earlier data so that the continuum is obviously lower than that chosen in earlier works where this higher strength could not be distinguished from the continuum or other processes. If the continuum is chosen approximately consistent with the earlier works, the slice analysis shows $86\pm 12\%$ of the $E2$ EWSR, in agreement with the folding analysis of the previous work.

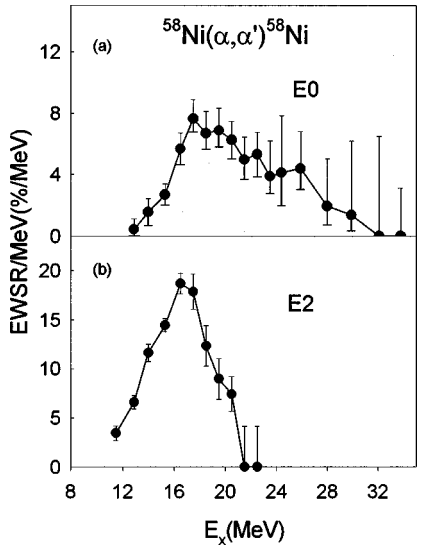

FIG. 3. (a) $E0$ strength distribution. (b) $E2$ strength distribution.

A total of 74^{+22}_{-12}% of the $E0$ EWSR was identified between $E_x = 12.0$ and 31.1 MeV with a centroid (m_1/m_0) of $20.30^{+1.69}_{-0.14}$ MeV and rms width of $4.25^{+0.69}_{-0.23}$ MeV. $(m_3/m_1)^{1/2}$ and $(m_1/m_{-1})^{1/2}$ are $21.48^{+3.01}_{-0.32}$ MeV and $19.93^{+1.34}_{-0.07}$ MeV, respectively. Of this, 13% of the $E0$ EWSR was found in the continuum. No $E0$ strength was identified above $E_x = 31.1$ MeV. In the region below $E_x = 25$ MeV, this work identified 58 ± 6% of the $E0$ EWSR, in agreement with the Satchler and Khoa analysis [2] of the previous work [1] where 50% was identified in the peaks. The +22% uncertainty in the total $E0$ strength arises because $E0$ cross sections are very small [4,5] at higher excitation energies and small undetected $E0$ cross section could contribute considerable strength, particularly above $E_x = 35$ MeV.

The uncertainty in the $E0$ and $E2$ strengths includes the experimental error and the error in the analysis but does not include uncertainties due to the choice of the continuum or those related to the DWBA calculations or differing models of the resonances that may lead to different transition densities. The $E0$ strength was extracted by fitting both the peak and the continuum, which was possible because of the strong 0° peaking of the $E0$ strength, a feature clearly absent in the continuum above $E_x = 35$ MeV. In analyses of these data with different choices of continuum ranging from the low one reported here to the high continuum used in the earlier analyses, the total $E0$ strength obtained (peak plus continuum) ranged from 74^{+20}_{-6}% (low continuum) to 80^{+20}_{-7}% (high continuum) where the errors are only those of the fitting procedure. Thus the $E0$ strength obtained is essentially independent of continuum choice. Unfortunately the $E2$ strength has no such unique signature and the continuum could contain considerable undetected $E2$ strength. Different choices of the continuum result in large differences in $E2$ strength (86% with the earlier high continuum to 115% with the lower continuum). In the absence of more definitive experiments (decay?) to better define the actual continuum, we choose not to assign a particular value to the uncertainty in $E2$ strength from the continuum choice. Unfortunately, there are still no reliable calculations for the continuum in inelastic scattering of 240-MeV α particles at small angles.

The model-dependent uncertainties were discussed at length by Satchler and Khoa [2]. We have verified for several nuclei that we agree with electromagnetic strengths for low-lying 2^+ and 3^- states [3,5,11] which suggests that the model dependence of the $E2$ strength may be small. However, there are no known low-lying $E0$ states with GMR transition densities to calibrate our results. The effects of random-phase approximation (RPA) transition densities have been explored by Chomaz *et al.* [14] for ^{40}Ca, ^{60}Ni, and ^{208}Pb for 152-MeV α scattering where they calculated cross sections using RPA transition densities and compared to those obtained with GMR transition density such as we used. Their conclusion was that $E0$ strength was underestimated about 10% in the usual collective model analysis. This is the subject of several current investigations.

The $E0$ strength located in ^{58}Ni is consistent with recent results for ^{40}Ca [5], ^{28}Si [4], and ^{24}Mg [3] where 92 ± 15%, 55 ± 20%, and 75 ± 15%, respectively, of the $E0$ EWSR has been identified in the region up to $E_x = 35$ MeV.

This work was supported in part by the Department of Energy under Grant No. DE-FG03-93ED40773 and by the Robert A. Welch Foundation.

[1] D. H. Youngblood, H. L. Clark, and Y.-W. Lui, Phys. Rev. Lett. **76**, 1429 (1996).
[2] G. R. Satchler and Dao T. Khoa, Phys. Rev. C **55**, 285 (1997).
[3] D. H. Youngblood, Y.-W. Lui, and H. L. Clark, Phys. Rev. C **60**, 014304 (1999).
[4] D. H. Youngblood, H. L. Clark, and Y.-W. Lui, Phys. Rev. C **57**, 1134 (1998).
[5] D. H. Youngblood, Y.-W. Lui, and H. L. Clark, Phys. Rev. C **55**, 2811 (1997).
[6] D. H. Youngblood, H. L. Clark, and Y.-W. Lui, Phys. Rev. Lett. **82**, 691 (1999).
[7] M. Rhoades-Brown, M. H. Macfarlane, and S. C. Pieper, Phys. Rev. C **21**, 2417 (1980); M. H. Macfarlane and S. C. Pieper, Argonne National Laboratory Report No. ANL-76-11, Rev. 1, 1978 (unpublished).
[8] G. R. Satchler, Nucl. Phys. **A540**, 533 (1992).
[9] L. D. Rickerston, The folding program DOLFIN, 1976 (unpublished).
[10] G. R. Satchler, Nucl. Phys. **A472**, 215 (1987).
[11] H. L. Clark, Y.-W. Lui, and D. H. Youngblood (unpublished).
[12] S. S. Dietrich and B. L. Berman, At. Data Nucl. Data Tables **38**, 199 (1988).
[13] D. H. Youngblood, Y.-W. Lui, U. Garg, and R. J. Peterson, Phys. Rev. C **45**, 2172 (1992).
[14] Ph. Chomaz, Tüna Suomijärvi, N. Van Giai, and J. Treiner, Phys. Lett. B **281**, 6 (1992).